1 **Virally derived peptide inhibitors of the herpes simplex virus type 1 nuclear egress complex**

2

3 *Elizabeth B. Draganova[1] and Ekaterina E. Heldwein[1,*]*

4 [1]Department of Molecular Biology and Microbiology, Tufts University School of Medicine,

5 Boston, MA, 02111, USA

6

7 [*]Correspondence: Ekaterina Heldwein, Tufts University School of Medicine, 136 Harrison

8 Avenue, Boston, MA 02111; 617-636-0858; katya.heldwein@tufts.edu

9

Abstract

Herpesviruses infect a majority of the human population, establishing lifelong latent infections for which there is no cure. Periodic viral reactivation spreads infection to new hosts while causing various disease states particularly detrimental in the immunocompromised. Efficient viral replication, and ultimately the spread of infection, is dependent on the nuclear egress complex (NEC), a conserved viral heterodimer that helps translocate mature viral capsids from the nucleus to the cytoplasm where they mature into infectious virions. Here, we have identified peptides capable of inhibiting NEC activity *in vitro*. Biophysical characterization of these peptides using circular dichroism suggests that secondary structure, rather than amino acid sequence, influences the extent of inhibition. Current therapeutics that target viral DNA replication machinery are rendered ineffective by drug resistance due to viral mutations. Our results establish a basis for the development of an alternative class of inhibitors against nuclear egress, an essential step in herpesvirus replication, potentially expanding the current repertoire of available therapeutics.

24 The design of novel antiviral therapeutics is a rapidly expanding field because viruses remain
25 one of the most common causes of human disease. One important group of viral human
26 pathogens are herpesviruses that infects a majority of the population by establishing lifelong
27 dormant infections for which there is no cure (reviewed in [1-3]). Periodically, the virus reactivates,
28 resulting in diseases such as keratitis, blindness, and cancers, which pose a significant threat to
29 immunocompromised individuals. Current antiviral treatments of choice are nucleoside analogs
30 such as acyclovir that target DNA replication machinery; yet, viral resistance to these drugs
31 renders them ineffective, highlighting the need for additional therapeutics[4-6].
32 The spread of infection to uninfected tissues and hosts relies on the ability of the virus to
33 effectively replicate[2,7]. During replication, viral capsids are assembled within the nucleus and
34 must translocate into the cytoplasm to form infectious virions but are too large to traverse
35 nuclear pores, and instead use an unusual route termed nuclear egress. The first step in this
36 process is the budding of a capsid at the inner nuclear membrane (INM), which is mediated by
37 the conserved nuclear egress complex (NEC), a heterodimer of viral proteins UL31 and UL34 [2,8].
38 The NEC is anchored to the INM by the single C-terminal transmembrane helix of UL34[9]. UL31
39 colocalizes with UL34[10,11] so that the complex extends outward into the nucleoplasm where
40 UL31 binds capsids ready for egress[12,13].
41 Our group has demonstrated that purified recombinant NEC expressed in *E. coli*
42 vesiculates synthetic membranes (giant unilamellar vesicles; GUVs) in the absence of other
43 proteins or ATP[14]. Using cryo-electron microscopy and tomography (cryo-EM/ET), we showed
44 that during budding, NEC oligomerizes into hexagonal membrane-bound coats[14]. We also found
45 that HSV-1 NEC formed a hexagonal lattice of similar dimensions in crystals, which reinforced
46 the inherent ability of the complex to form hexagonal arrays and provided an atomic-level view

47 of protein interactions within the coat[15]. Mutations intended to disrupt hexagonal lattice

48 formation impaired NEC-mediated budding *in vitro* and reduced nuclear egress and viral

49 replication *in vivo*[16,17], which confirmed that NEC oligomerization is essential for the NEC

50 function. Furthermore, removal of NEC regions required for binding membranes *in vitro*[14] also

51 reduced viral replication *in vivo*[18,19], suggesting that appropriate membrane interactions are also

52 required for budding. Therefore, NEC-mediated budding is as an attractive therapeutic target.

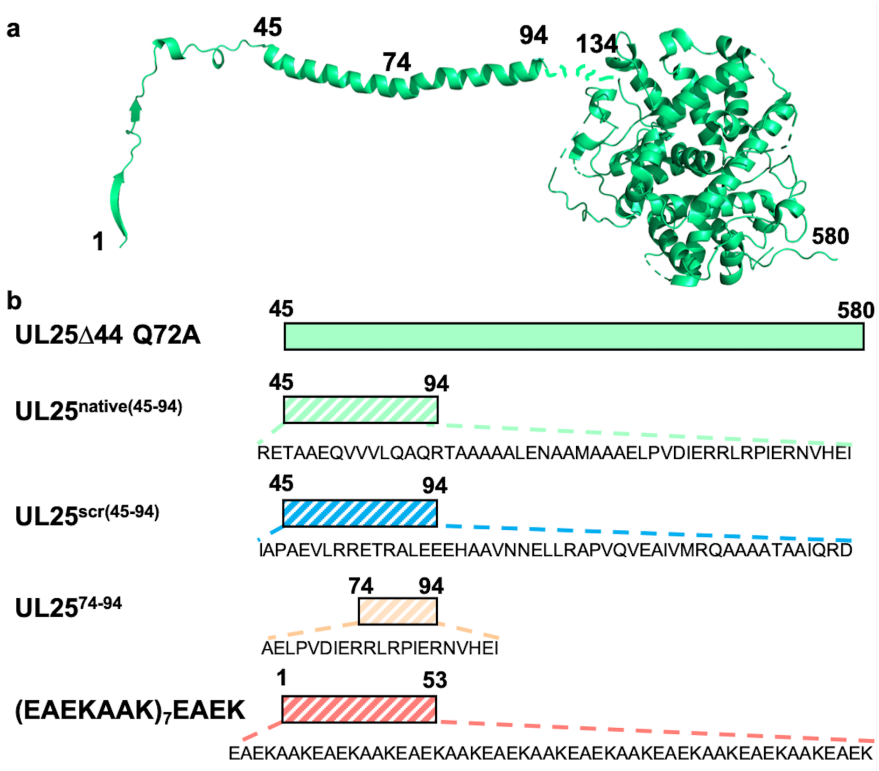

53

54 **Figure 1. UL25-based peptide design. a)** The structure of full length capsid-bound HSV-1 UL25 [residues 1-
55 94 determined by cryoEM; residues 134-580 determined by x-ray crystallography (PDB code: 2F5U)]. **b)**
56 Schematics of peptides and protein constructs used in NEC-inhibition studies. Peptides are indicated by stripes.
57 Amino acid sequences of each peptide are given below each schematic. UL25$^{native(45-94)}$: the native N-terminal
58 helix of UL25; UL25$^{scr(45-94)}$: the amino acid sequence of UL25$^{native(45-94)}$ scrambled; UL25$^{74-94}$: the C-terminal
59 half of the UL25$^{native(45-94)}$ peptide; $(EAEKAAK)_7EAEK$: a well-characterized α-helical peptide made of
60 EAEKAAK repeats.

61

62 Recently, we showed that HSV-1 NEC-mediated budding could be inhibited *in vitro* by

63 another HSV-1 protein, capsid protein UL25[20]. UL25 is located at the capsid vertices and is

64 thought to anchor the NEC to the capsid during nuclear egress[13,21]. We found that an N-

65 terminally truncated UL25 construct UL25Δ44 Q72A (Fig. 1) inhibited NEC budding at a 10:1
66 molar ratio of UL25:NEC[20]. Using cryo-ET, we showed that the observed inhibitory effect on
67 NEC budding correlated with a network of interconnected UL25 stars formed on top of the
68 membrane-bound NEC layer. We hypothesized that this UL25 network blocked budding by
69 preventing the conformational changes within the NEC necessary to generate membrane
70 deformation and budding. UL25-mediated budding inhibition required the N-terminal α-helix in
71 UL25, residues 45-94 (Fig. 1a), as a UL25Δ73 construct in which the N-terminal ~1/2 of this
72 helix was truncated did not inhibit budding. We then tested whether peptides derived from the N-
73 terminal α-helix of UL25 could inhibit NEC-mediated budding. Here, we show that UL25-
74 derived peptides inhibit NEC budding and identify structural characteristics essential for
75 inhibition.
76
77 **Results**
78 **Full-length UL25 derived peptides inhibit NEC budding regardless of sequence.** We first
79 tested whether the peptide corresponding to the entire N-terminal helix of UL25, $UL25^{native(45-94)}$
80 (Fig. 1b), inhibited NEC-mediated budding in a well-established *in vitro* GUV budding assay[14]
81 (Fig. 2). At a 1:10 molar ratio of NEC:peptide (the same inhibitory ratio as used with the UL25
82 protein), the $UL25^{native(45-94)}$ peptide inhibited NEC budding by ~80%, nearly as efficiently as the
83 UL25Δ44 Q72A construct (~90% inhibition) (Fig. 2). Surprisingly, a scrambled $UL25^{scr(45-94)}$
84 peptide (Fig. 1b) inhibited budding by ~80%, nearly as efficiently as the $UL25^{native(45-94)}$ peptide
85 (Fig. 2). This suggested that the native UL25 peptide sequence was unimportant for the
86 inhibitory activity.

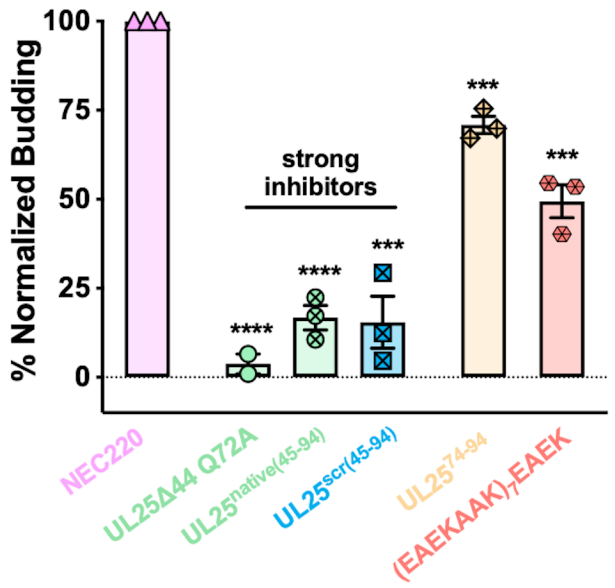

Figure 2. Specific peptides inhibit NEC budding. The UL25$^{native(45-94)}$ and UL25$^{scr(45-94)}$ peptides inhibit NEC-mediated budding whereas the UL25$^{74-94}$ peptide does not. The α-helical $(EAEKAAK)_7EAEK$ peptide only partially inhibits NEC-mediated budding. Budding was tested at 1:10 molar ratios of either NEC:UL25 or NEC:peptide. Each construct/peptide was tested in at least two biological replicates, each consisting of three technical replicates. Symbols represent average budding efficiency of at least two biological replicates relative to NEC220 (100%). Error bars represent the standard error of measurement for at least two individual experiments. Significance compared to NEC220 was calculated using an unpaired t-test. ***P-value < 0.001 and ****P-value < 0.0001.

α-helical formation may be important for peptide-mediated NEC budding inhibition. Both the UL25$^{native(45-94)}$ and UL25$^{scr(45-94)}$ peptides were only ~15% α-helical in solution (Fig. 3a, b) according to the circular dichroism (CD) estimates using DichroWeb[22] (Supplementary Table S1). However, within capsid-bound UL25, amino acids 48-94 form an α-helix (Fig. 1a), which suggested that this sequence has a propensity to form α-helical structure under certain conditions. Therefore, the CD experiment with the UL25$^{native(45-94)}$ and UL25$^{scr(45-94)}$ peptides was repeated in the presence of 30% trifluoroethanol (TFE) known to stabilize secondary structure[23]. Both peptides adopted α-helical structure (~50% and ~75%, respectively) in the presence of TFE (Fig. 3a, b) suggesting that each peptide could, in principle, form an α-helix in the right environment, for example, when bound to a protein partner such as the NEC. The $\theta_{222}/\theta_{208}$ ratios

107 of these peptides either in the absence or presence of TFE were less than 0.9 indicating peptides

108 were forming individual helices rather than coiled coils[24].

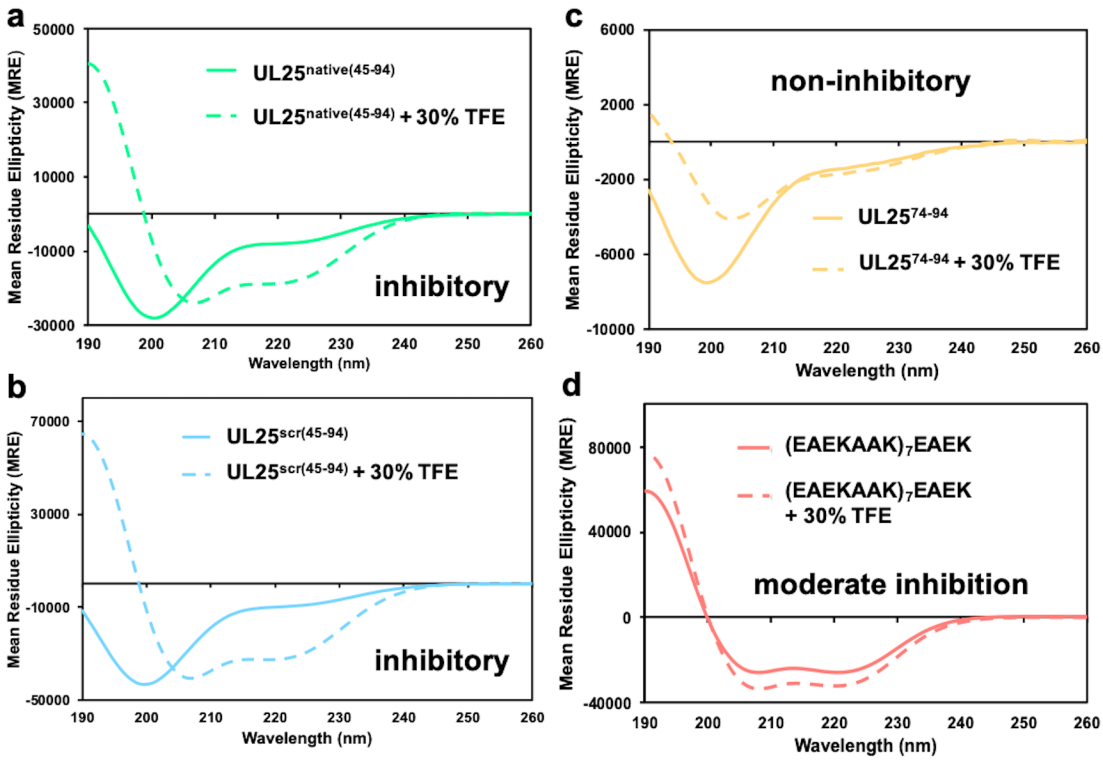

109

110 **Figure 3. α-helical formation is important for NEC budding inhibition. a-d)** Far-UV CD spectra of each
111 peptide with (dashed lines) and without (solid lines) 30% TFE. Both the $UL25^{native(45-94)}$ and the $UL25^{scr(45-94)}$
112 peptides exist as random coils which can form α-helices in the presence of 30% TFE and inhibit NEC budding.
113 Alternatively, $UL25^{74-94}$ can only form a random coil and cannot inhibit NEC budding. The
114 $(EAEKAAK)_7EAEK$ peptide is α-helical, regardless of the presence of TFE, and only moderately inhibits
115 budding, suggesting a pre-formed α-helical peptide precludes proper inhibitory contacts with the NEC.

116 We next tested a shorter $UL25^{74-94}$ peptide (Fig. 1b) and found that it did not inhibit

117 budding (Fig. 2). According to the CD analysis, the $UL25^{74-94}$ peptide adopted a random-coil

118 conformation in solution even in the presence of 30% TFE (Fig. 3c, Supplementary Table 1).

119 Therefore, the $UL25^{74-94}$ peptide may be unable to inhibit NEC budding because it cannot form

120 an α-helix.

121

122 **A pre-formed α-helical peptide moderately inhibits budding**. To determine if any α-helical

123 peptide of similar length to $UL25^{native(45-94)}$ could inhibit NEC-mediated budding, we generated a

124 heterologous 53-amino-acid peptide containing a series of well-characterized α-helical
125 EAEKAAK repeats [$(EAEKAAK)_7EAEK$][25]. The $(EAEKAAK)_7EAEK$ peptide inhibited NEC-
126 mediated budding but with a lower efficiency than either the $UL25^{native(45-94)}$ or the $UL25^{scr(45-94)}$
127 peptides, only by ~50% (Fig. 2). The moderate inhibitory activity of the $(EAEKAAK)_7EAEK$
128 peptide could be due to a different amino acid composition, notably, 60% charged residues
129 (glutamates and lysines) relative to the 30% charged residues (aspartates, glutamates and
130 arginines) in the UL25 inhibitory peptides. Additionally, the $(EAEKAAK)_7EAEK$ peptide was
131 60% α-helical in solution even in the absence of TFE (Fig. 3d, Supplementary Table 1), in
132 contrast to both the $UL25^{native(45-94)}$ and the $UL25^{scr(45-94)}$ peptides that became mostly α-helical
133 only in the presence of TFE (Fig. 3a, b). This observation suggested that while the inhibitory
134 peptide should be α-helical, instead of being a stable, pre-formed α-helix, it may need to form in
135 the presence of the NEC, in an induced-fit manner, for optimal inhibition.
136
137 **Peptides do not bind acidic membranes.** None of the peptides used in this study bound
138 multilamellar vesicles (MLVs) of the same lipid composition as the GUVs used in the budding
139 assay (Supplementary Fig. S1), which suggested that the peptides do not compete with the NEC
140 for binding to membranes. Therefore, we hypothesize that the peptides instead bind the NEC and
141 block its membrane-budding activity.
142
143 **Discussion**
144 Here, we have shown that two peptides derived from the N-terminal α-helix of UL25
145 efficiently inhibited NEC-mediated budding *in vitro*. A shorter UL25-derived peptide did not
146 inhibit budding whereas a heterologous α-helical peptide [$(EAEKAAK)_7EAEK$)] inhibited

147 budding with moderate efficiency. We hypothesize that the inhibitory ability of the peptides
148 depends more on their length and the ability to form an α-helix than the exact amino acid
149 sequence.

150 Peptide length was more important for inhibition than the sequence because 50-amino-
151 acid UL25 peptides, be they native or scrambled ($UL25^{native(45-94)}$ and $UL25^{scr(45-94)}$), efficiently
152 inhibited budding whereas the 21-amino-acid native peptide $UL25^{74-94}$ did not (Fig. 2). Future
153 studies will identify the minimal UL25 peptide length required for inhibition. The inhibitory
154 ability of UL25 peptides correlated not only with their length but also with the propensity to
155 adopt α-helical structure. Although all three UL25-derived peptides formed random coils in
156 solution, only the two 50-amino acid peptides formed α-helices in the presence of TFE. Thus, we
157 hypothesize that inhibitory peptides may need to be α-helical. The inability of $UL25^{74-94}$ to form
158 an α-helix could be due to the lower content of alanine and leucine residues, two amino acid
159 types with the highest propensity to form α-helices[26]. $UL25^{74-94}$ has 1% alanines and 2% leucines
160 whereas both $UL25^{native(45-94)}$ and $UL25^{scr(45-94)}$ have 26% and 8%, respectively.

161 The $(EAEKAAK)_7EAEK$ peptide, a 53-residue α-helical peptide of heterologous
162 sequence was also inhibitory but less so than the 50-residue UL25 peptides. This peptide is more
163 highly charged than the UL25 peptides and is α-helical in solution even in the absence of TFE. It
164 is possible that a stable, preformed α-helix may not be able to form appropriate inhibitory
165 contacts with the NEC and that for efficient inhibition, an α-helix of a specific length and amino-
166 acid content should form in the presence of the NEC, in an induced-fit manner. Alternatively, the
167 reduced inhibitory activity of the heterologous $(EAEKAAK)_7EAEK$ peptide could be due to
168 differences in the amino-acid composition. This peptide forms an amphipathic α-helix with a
169 highly charged face rich in glutamates and lysines and a hydrophobic face rich in alanines

170 (Supplementary Fig. S2) that could bind the NEC in a different manner compared to the
171 inhibitory peptides, leading to partial budding inhibition. In contrast, inhibitory UL25-derived
172 peptides have fewer charged residues and form α-helices with a less pronounced amphipathic
173 character (Supplementary Fig. S2). Therefore, future design of NEC peptide inhibitors should
174 take both of these characteristics into consideration.

175 The mechanism by which the inhibitory peptides inhibit budding is yet unclear. None of
176 the peptides bound membranes, which ruled out competition with the NEC for binding to
177 membranes. Therefore, we hypothesize that the peptides must instead inhibit the activity of the
178 NEC by binding it directly. Our previous study suggested that UL25 inhibited NEC-mediated
179 budding by oligomerizing into a network of interconnected stars on top of the membrane-bound
180 NEC layer as observed by cryo-ET[20]. We hypothesized that the N-terminal helices link the
181 neighboring UL25 molecules into a network by forming antiparallel helical bundles that
182 sterically blocked the NEC from undergoing conformational changes necessary for membrane
183 budding. Both the N-terminal helix and the C-terminal core of UL25 (Fig. 1a) were important for
184 inhibition. However, the inhibitory UL25 peptides in our current study were composed of only
185 the N-terminal helix. Therefore, they likely bind the NEC differently from UL25 and use a
186 different mechanism to inhibit budding. Being much smaller than UL25, the inhibitory peptides
187 can interact with the NEC at sites otherwise inaccessible to the UL25 protein.

188 One possibility is that the inhibitory peptides bind the NEC and prevent its binding to
189 membranes. Membrane binding of the NEC is thought to rely on electrostatic interactions
190 between the membrane-binding regions rich in basic residues and acidic membranes[14]. Both
191 $UL25^{native(45-94)}$ and $UL25^{scr(45-94)}$ have acidic residues (8 glutamates and 1 aspartate). Modeling
192 these peptides as helices suggests some of these residues could form acidic patches

193 (Supplementary Fig. S3) which may potentially interact with NEC regions required for efficient

194 membrane binding to inhibit budding. Alternatively, NEC/peptide interactions may block

195 NEC/NEC interactions necessary for the assembly of the hexagonal NEC coat thereby blocking

196 the induction of negative curvature and, ultimately, budding (Fig. 4).

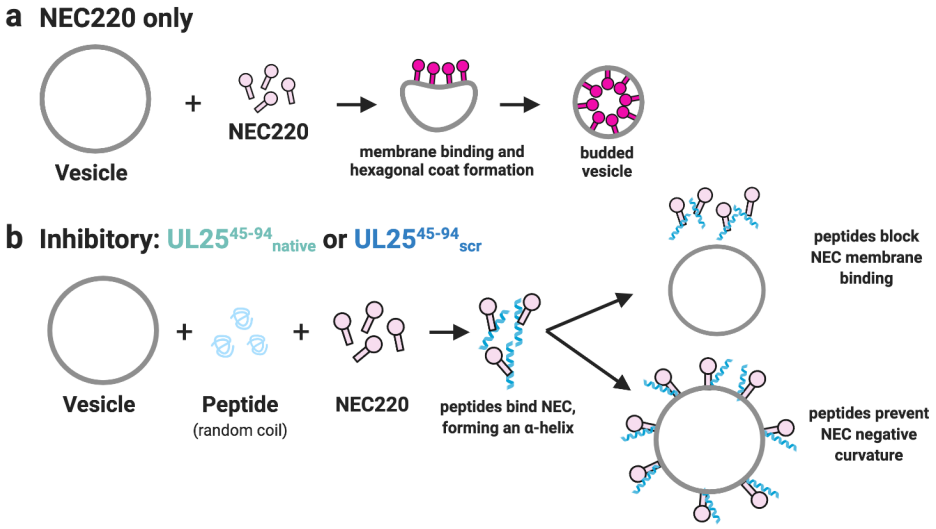

197

198 **Figure 4.** Proposed models of peptide-mediated NEC budding inhibition. **a)** NEC (pink) alone forms a
199 hexagonal coat on membranes (magenta) which induces negative curvature forming a budded vesicle. **b)** Both
200 $UL25^{native(45-94)}$ and $UL25^{scr(45-94)}$ (blue/green) inhibit budding by forming α-helices upon binding to the NEC,
201 inhibiting binding of NEC to membranes. Alternatively, NEC binds membranes and inhibitory peptides
202 prevent coat formation and ultimately, conformational changes needed for negative curvature. This figure was
203 created with Biorender.com.

204 Regardless of the precise mechanism, our results suggest that inhibitory peptides should

205 be of a certain length, moderately charged, and unstructured in solution, yet capable of forming

206 α-helical structure, presumably, upon binding to the NEC. Alternatively, inhibitory random coil

207 peptides may be sufficient for budding inhibition without the requirement of α-helical formation.

208 Short peptides incapable of forming an α-helical structure do not inhibit budding whereas

209 charged peptides that form a stable α-helix on their own inhibit budding inefficiently. Further

210 structural analyses of the inhibitory peptides in the presence of the NEC are necessary to narrow

211 down the optimal characteristics of the inhibitory peptides.

212 Efficient NEC function is required for successful replication of herpesviruses. To our
213 knowledge, this is the first study reporting a peptide-based approach targeting NEC budding. Our
214 work provides a starting point for the rational design of peptide-based inhibitors of the NEC and
215 nuclear egress. Both the NEC and UL25 are conserved across all herpesviruses raising an
216 intriguing possibility that UL25-derived peptides could be used to inhibit NEC homologs from
217 other herpesviruses.
218

219 **Materials and Methods**

220 ***Cloning.*** All primers used in cloning are listed in Supplementary Table S2. DNA sequences
221 encoding each peptide were subcloned into the prokaryotic expression vector pGEX-6P-1 that
222 encodes a N-terminal GST-tag followed by a PreScission Protease cleavage site in frame with
223 the BamHI restriction site within the multiple cloning site. Both the $UL25^{native(45-94)}$ and $UL25^{74-94}$
224 peptide DNA sequences were amplified by PCR from pED03 (UL25Δ44 Q72A) and subcloned
225 into the pGEX-6P-1 vector using restriction digest via BamHI and XhoI to create the pED23
226 [$UL25^{native(45-94)}$] and pED38 ($UL25^{74-94}$) plasmids. Both the scrambled [$UL25^{scr(45-94)}$] and α-
227 helical [$(EAEKAAK_7)EAEK$] peptide DNA sequences were obtained as a gBlock gene fragment
228 (IDT) and subjected to restriction digest cloning with BamHI and XhoI into the pGEX-6P-1
229 vector (gene fragment sequences are given in Supplementary Table S2) to create the pED34
230 ($UL25^{scr(45-94)}$ peptide) and pED39 [$(EAEKAAK_7)EAEK$ peptide] plasmids.
231

232 ***Expression and purification of NEC220.*** Plasmids encoding HSV-1 UL31 1-306 (pKH90) and
233 UL34 1-220 (pJB02) were co-transformed into *Escherichia coli* BL21(DE3) LoBSTr cells
234 (Kerafast) to generate NEC220 (NEC construct absent of the UL34 C-terminal transmembrane

235 helix)[14]. NEC220 was expressed using autoinduction at 37 °C in Terrific Broth (TB)
236 supplemented with 100 μg/mL kanamycin, 100 μg/mL ampicillin, 0.2% lactose and 2 mM
237 $MgSO_4$ for 4 h. The temperature was then reduced to 25 °C for 16 h. Cells were harvested at
238 5,000 x g for 30 min. NEC220 was purified as previously described[14] with slight modifications.
239 NEC220 was passed over 2 x 1 mL HiTrap Talon columns (GE Healthcare), rather than ion
240 exchange as previously described, to remove excess cleaved His_6-SUMO before injection onto
241 size-exclusion chromatography (as previously described).
242
243 ***Expression and purification of peptides.*** Plasmids encoding the peptide sequences were
244 expressed and cells harvested as described above for the NEC220. Cells were resuspended in
245 lysis buffer (50 mM Na HEPES pH 7.5, 500 mM NaCl, 1 mM TCEP, and 10% glycerol) plus
246 Complete protease inhibitor (Roche) and lysed using a microfluidizer 110S (Microfluidics). The
247 cell lysate was centrifuged at 13,000 x g for 35 min, and the supernatant passed over a
248 Glutathione sepharose 4B (GE Healthcare) column, which was subsequently washed with lysis
249 buffer. The GST-tag was cleaved on the glutathione sepharose column for 16 h using the
250 PreScission Protease described above. Peptides were eluted off the column with lysis buffer. As
251 a final purification step, peptides were purified with size-exclusion chromatography using a
252 Superdex 75 column (GE Healthcare) equilibrated with 20 mM Na HEPES, pH 7.0, 100 mM
253 NaCl, and 1 mM TCEP (for budding assays) or with 10 mM sodium phosphate, pH 7.4, and 100
254 mM NaF (for CD studies). Absorbance was monitored at 214 nm because the peptides lack
255 aromatic residues. The peptides were purified to homogeneity as assessed by both 16.5% Tris-
256 Tricine SDS-PAGE and 12% SDS-PAGE with Coomassie staining. Fractions containing peptide

257 were concentrated and sent off for amino acid analysis (University of Colorado Denver Anschutz
258 Medical Campus) for accurate concentration determination.
259
260 ***Co-sedimentation assay.*** Co-sedimentation of peptides to acidic multilamellar vesicles (MLVs)
261 was performed as previously described[14]. MLVs were prepared in a 3:1:1 ratio of 1-palmitoyl-2-
262 oleoyl-glycero-3-phosphocholine (POPC):1-palmitoyl-2-oleoyl-sn-glycero-3-phospho-L-serine
263 (POPS):1-palmitoyl-2-oleoyl-sn-glycero-3-phosphate (POPA) (Avanti Polar Lipids).
264 Background signal in the absence of liposomes is due to protein aggregation during
265 centrifugation. The reported values represent the percentage (0-100 %) of either NEC220 or
266 peptide bound to membranes. The standard error of the mean is reported for each measurement.
267 Each condition was tested in one biological replicate with two technical replicates.
268
269 ***GUV Budding Assays.*** Giant unilamellar vesicles (GUVs) were prepared as previously
270 described[14]. For NEC220 only budding quantification, a total of 10 μL of GUVs with a 3:1:1
271 ratio of POPC:POPS:POPA containing ATTO-594 DOPE (ATTO-TEC GmbH) at a
272 concentration of 0.2 μg/μL was mixed with 1 μM NEC220 (final concentration), and 0.2 mg/mL
273 (final concentration) Cascade Blue Hydrazide (ThermoFisher Scientific). For the NEC and
274 peptide experiments, 10 μL of GUVs and 10 μM (final concentration) of either the $UL25^{native(45-}$
275 $^{94)}$, $UL25^{scr(45-94)}$, $UL25^{74-94}$, or $(EAEKAAK)_7EAEK$ peptides were incubated with 1 μM of
276 NEC220 (final concentration) along with Cascade blue. The total volume of each sample during
277 imaging for all experiments was brought to 100 μL with gel filtration buffer and the reaction was
278 incubated for 5 min at 20 °C. Samples were imaged in a 96-well chambered cover-glass. Images
279 were acquired using a Nikon A1R Confocal Microscope with a 60x oil immersion lens at the

280 Tufts Imaging Facility in the Center for Neuroscience Research at Tufts University School of
281 Medicine. Quantification was performed by counting vesicles in 15 different frames of the
282 sample (~300 vesicles total). Each condition was tested in at least two biological replicates. Prior
283 to analysis, the background was subtracted from the raw values. The reported values represent
284 the average budding activity relative to NEC220 (100%). The standard error of the mean is
285 reported for each measurement. Significance compared to NEC220 was calculated using an
286 unpaired one-tailed *t*-test against NEC220.
287
288 ***Circular dichroism (CD) studies.*** Far-UV CD spectra of peptides (0.1 mg/mL) were recorded in
289 10 mM Na phosphate, pH 7.4, and 100 mM NaF buffer using a Jasco 815 CD Spectropolarimeter
290 at the Center for Macromolecular Interactions at Harvard Medical School. Peptide spectra were
291 also measured in the presence of 30% trifluoroethanol (TFE). Data were collected at ambient
292 temperature with a scan speed of 50 nm/min and 5 accumulations of each sample was averaged.
293 The raw data was blank subtracted and converted to mean residue ellipticity (MRE). Helical
294 content was estimated using DichroWeb[22] and average values from three reference datasets
295 generated by the same analysis program are provided in Supplementary Table S1.
296

297 **References**
298

299 1. Johnson, D. C. & Baines, J. D. Herpesviruses remodel host membranes for virus egress.
300 *Nat. Rev. Microbiol.* **9**, 382-394, doi:10.1038/nrmicro2559 (2011).

301 2. Bigalke, J. M. & Heldwein, E. E. Nuclear exodus: Herpesviruses lead the way. *Annu.*
302 *Rev. Virol.* **3**, 387-409, doi:10.1146/annurev-virology-110615-042215 (2016).

303 3. Mettenleiter, T. C., Klupp, B. G. & Granzow, H. Herpesvirus assembly: an update. *Virus*
304 *Res.* **143**, 222-234, doi:10.1016/j.virusres.2009.03.018 (2009).

305 4. Szczubialka, K., Pyrc, K. & Nowakowska, M. In search for effective and definitive
306 treatment of herpes simplex virus type 1 (HSV-1) infections. *RSC Adv.* **6**, 1058-1075,
307 doi:10.1039/c5ra22896d (2016).

308 5. Engel, J. P., Englund, J. A., Fletcher, C. V. & Hill, E. L. Treatment of resistant herpes
309 simplex virus with continuous-infusion acyclovir. *JAMA.* **263**, 1662-1664 (1990).

310 6. Antoine, T. E., Park, P. J. & Shukla, D. Glycoprotein targeted therapeutics: a new era of
311 anti-herpes simplex virus-1 therapeutics. *Rev. Med. Virol.* **23**, 194-208,
312 doi:10.1002/rmv.1740 (2013).

313 7. Roller, R. J. & Baines, J. D. in *Adv. Anat. Embryol. Cell. Biol.* Vol. 223 (ed Klaus
314 Osteirrieder) Ch. 7, 143-169 (Springer, 2017).

315 8. Reynolds, A. E., Wills, E. G., Roller, R. J., Ryckman, B. J. & Baines, J. D. Ultrastructural
316 localization of the herpes simplex virus type 1 UL31, UL34, and US3 proteins suggests
317 specific roles in primary envelopment and egress of nucleocapsids. *J. Virol.* **76**, 8939-
318 8952 (2002).

319 9. Shiba, C. *et al.* The UL34 gene product of herpes simplex virus type 2 is a tail-anchored
320 type II membrane protein that is significant for virus envelopment. *J. Gen. Virol.* **81**,
321 2397-2405, doi:10.1099/0022-1317-81-10-2397 (2000).

322 10. Reynolds, A. E. *et al.* U(L)31 and U(L)34 proteins of herpes simplex virus type 1 form a
323 complex that accumulates at the nuclear rim and is required for envelopment of
324 nucleocapsids. *J. Virol.* **75**, 8803-8817 (2001).

325 11. Chang, Y. E. & Roizman, B. The product of the UL31 gene of herpes simplex virus 1 is a
326 nuclear phosphoprotein which partitions with the nuclear matrix. *J. Virol.* **67**, 6348-6356
327 (1993).

328 12. Trus, B. L. *et al.* Allosteric signaling and a nuclear exit strategy: binding of UL25/UL17
329 heterodimers to DNA-Filled HSV-1 capsids. *Mol. Cell.* **26**, 479-489,
330 doi:10.1016/j.molcel.2007.04.010 (2007).

331 13. Yang, K. & Baines, J. D. Selection of HSV capsids for envelopment involves interaction
332 between capsid surface components pUL31, pUL17, and pUL25. *Proc. Natl. Acad. Sci.*
333 **108**, 14276-14281, doi:10.1073/pnas.1108564108 (2011).

334 14. Bigalke, J. M., Heuser, T., Nicastro, D. & Heldwein, E. E. Membrane deformation and
335 scission by the HSV-1 nuclear egress complex. *Nat. Commun.* **5**, 4131,
336 doi:10.1038/ncomms5131 (2014).

337 15. Bigalke, J. M. & Heldwein, E. E. Structural basis of membrane budding by the nuclear
338 egress complex of herpesviruses. *EMBO J.* **34**, 2921-2936,
339 doi:10.15252/embj.201592359 (2015).

340 16. Roller, R. J., Zhou, Y., Schnetzer, R., Ferguson, J. & DeSalvo, D. Herpes simplex virus
341 type 1 U(L)34 gene product is required for viral envelopment. *J. Virol.* **74**, 117-129
342 (2000).

343 17. Fuchs, W., Klupp, B. G., Granzow, H., Osterrieder, N. & Mettenleiter, T. C. The
344 interacting UL31 and UL34 gene products of pseudorabies virus are involved in egress
345 from the host-cell nucleus and represent components of primary enveloped but not
346 mature virions. *J. Virol.* **76**, 364-378 (2002).

347 18. Mou, F., Wills, E. & Baines, J. D. Phosphorylation of the U(L)31 protein of herpes
348 simplex virus 1 by the U(S)3-encoded kinase regulates localization of the nuclear
349 envelopment complex and egress of nucleocapsids. *J. Virol.* **83**, 5181-5191,
350 doi:10.1128/jvi.00090-09 (2009).

351 19. Passvogel, L., Trube, P., Schuster, F., Klupp, B. G. & Mettenleiter, T. C. Mapping of
352 sequences in Pseudorabies virus pUL34 that are required for formation and function of
353 the nuclear egress complex. *J. Virol.* **87**, 4475-4485, doi:10.1128/jvi.00021-13 (2013).

354 20. Draganova, E. B., Zhang, J., Zhou, Z. H. & Heldwein, E. E. Structural basis for capsid
355 recruitment and coat formation during HSV-1 nuclear egress. Preprint at
356 https://www.biorxiv.org/content/10.1101/2020.03.11.988170v1.full (2020).

357 21. Yang, K., Wills, E., Lim, H. Y., Zhou, Z. H. & Baines, J. D. Association of herpes
358 simplex virus pUL31 with capsid vertices and components of the capsid vertex-specific
359 complex. *J. Virol.* **88**, 3815-3825, doi:10.1128/jvi.03175-13 (2014).

360 22. Whitmore, L. & Wallace, B. A. Protein secondary structure analyses from circular
361 dichroism spectroscopy: methods and reference databases. *Biopolymers.* **89**, 392-400,
362 doi:10.1002/bip.20853 (2008).

363 23. Luo, P. & Baldwin, R. L. Mechanism of helix induction by trifluoroethanol: a framework
364 for extrapolating the helix-forming properties of peptides from trifluoroethanol/water
365 mixtures back to water. *Biochemistry.* **36**, 8413-8421, doi:10.1021/bi9707133 (1997).

366 24. Lau, S. Y., Taneja, A. K. & Hodges, R. S. Synthesis of a model protein of defined
367 secondary and quaternary structure. Effect of chain length on the stabilization and

formation of two-stranded alpha-helical coiled-coils. *J. Biol. Chem.* **259**, 13253-13261 (1984).

25. Zhou, N. E., Kay, C. M., Sykes, B. D. & Hodges, R. S. A single-stranded amphipathic alpha-helix in aqueous solution: design, structural characterization, and its application for determining alpha-helical propensities of amino acids. *Biochemistry*. **32**, 6190-6197 (1993).

26. Pace, C. N. & Scholtz, J. M. A helix propensity scale based on experimental studies of peptides and proteins. *Biophys. J.* **75**, 422-427 (1998).

378 **Acknowledgments**

379 We would like to thank Shaun Bevers (University of Colorado Denver Biophysics Core) for
380 performing amino acid analysis on the peptides. We also thank Peter Cherepanov (Francis Crick
381 Institute) for the gift of the GST-PreScission protease expression plasmid and Thomas Schwartz
382 (Massachusetts Institute of Technology) for the gift of LoBSTr cells. CD experiments were
383 performed at the Center for Macromolecular Interactions in the Department of Biological
384 Chemistry and Molecular Pharmacology at Harvard Medical School. This work was funded by
385 the NIH grants R01GM111795 and R01AI147625 (E.E.H.), a Faculty Scholar grant 55108533
386 from Howard Hughes Medical Institute (E.E.H.), and NIH postdoctoral fellowship
387 F32GM126760 (E.B.D.).

388

389 **Author Contributions**

390 E.B.D. and E.E.H. designed the experiments; E.B.D. performed all experiments and analyses
391 under the guidance of E.E.H; E.B.D. and E.E.H. wrote and reviewed the manuscript.

392

393 **Additional Information**

394 **Competing Interests:** The authors declare no competing interests.

395 **Figure 1. UL25-based peptide design. a)** The structure of full length capsid-bound HSV-1
396 UL25 [residues 1-94 determined by cryoEM; residues 134-580 determined by x-ray
397 crystallography (PDB code: 2F5U)]. **b)** Schematics of peptides and protein constructs used in
398 NEC-inhibition studies. Peptides are indicated by stripes. Amino acid sequences of each peptide
399 are given below each schematic. $UL25^{native(45-94)}$: the native N-terminal helix of UL25; $UL25^{scr(45-}$
400 $^{94)}$: the amino acid sequence of $UL25^{native(45-94)}$ scrambled; $UL25^{74-94}$: the C-terminal half of the

401 UL25$^{native(45-94)}$ peptide; $(EAEKAAK)_7EAEK$: a well-characterized α-helical peptide made of

402 EAEKAAK repeats.

403

404 **Figure 2. Specific peptides inhibit NEC budding.** The UL25$^{native(45-94)}$ and UL25$^{scr(45-94)}$ peptides

405 inhibit NEC-mediated budding whereas the UL2574-94 peptide does not. The α-helical

406 $(EAEKAAK)_7EAEK$ peptide only partially inhibits NEC-mediated budding. Budding was tested

407 at 1:10 molar ratios of either NEC:UL25 or NEC:peptide. Each construct/peptide was tested in at

408 least two biological replicates, each consisting of three technical replicates. Symbols represent

409 average budding efficiency of at least two biological replicates relative to NEC220 (100%). Error

410 bars represent the standard error of measurement for at least two individual experiments.

411 Significance compared to NEC220 was calculated using an unpaired t-test. ***P-value < 0.001

412 and ****P-value < 0.0001.

413

414 **Figure 3. α-helical formation is important for NEC budding inhibition. a-d)** Far-UV CD

415 spectra of each peptide with (dashed lines) and without (solid lines) 30% TFE. Both the

416 UL25$^{native(45-94)}$ and the UL25$^{scr(45-94)}$ peptides exist as random coils which can form α-helices in the

417 presence of 30% TFE and inhibit NEC budding. Alternatively, UL25$^{74-94}$ can only form a random

418 coil and cannot inhibit NEC budding. The $(EAEKAAK)_7EAEK$ peptide is α-helical, regardless

419 of the presence of TFE, and only moderately inhibits budding, suggesting a pre-formed α-helical

420 peptide precludes proper inhibitory contacts with the NEC.

421

422 **Figure 4. Proposed models of peptide-mediated NEC budding inhibition. a)** NEC (pink)

423 alone forms a hexagonal coat on membranes (magenta) which induces negative curvature

forming a budded vesicle. **b)** Both $UL25^{native(45-94)}$ and $UL25^{scr(45-94)}$ (blue/green) inhibit budding by forming α-helices upon binding to the NEC, inhibiting binding of NEC to membranes. Alternatively, NEC binds membranes and inhibitory peptides prevent coat formation and ultimately, conformational changes needed for negative curvature. This figure was created with Biorender.com.